

# Designing a Green Roof for Ireland

**Report Contributors:** Ian Hewitt<sup>1</sup>, Andrew Lacey<sup>2</sup>,  
Niklas Mellgren<sup>3</sup>, Michael Vynnycky<sup>4</sup>,  
Marguerite Robinson<sup>4,5</sup> and Mark Cooker<sup>6</sup>

**Study Group Contributors:** Andrew Fowler<sup>4</sup>, Maria Gonzalez<sup>4</sup>,  
Hilda Simboek<sup>4</sup>, Thomas Murphy<sup>7</sup>, Michael Devereux<sup>4</sup>, Roman  
Sedakov<sup>4</sup>, Grainne Kirby<sup>4</sup>, Gemma Fay<sup>1</sup> and Qi Wang<sup>8</sup>

**Industry Representatives:**

Catherine Adley<sup>7</sup>, Billy Kirwan<sup>9</sup> and John O'Hara<sup>10</sup>

---

<sup>1</sup>OCIAM, Mathematical Institute, University of Oxford, United Kingdom

<sup>2</sup>Department of Mathematics, University Heriot-Watt, United Kingdom

<sup>3</sup>Department of Mechanics, KTH Royal Institute of Technology, Sweden

<sup>4</sup>MACSI, Department of Mathematics and Statistics, University of Limerick, Ireland

<sup>5</sup>Report coordinator, marguerite.robinson@ul.ie

<sup>6</sup>School of Mathematics, University of East Anglia, United Kingdom

<sup>7</sup>Department of Chemical and Environmental Science, University of Limerick, Ireland

<sup>8</sup>School of mathematical sciences, Dublin Institute of Technology, Ireland

<sup>9</sup>GFM Systems, Waterway House, Crag Crescent, Clondalkin Ind. Estate, Dublin 22, Ireland

<sup>10</sup>Landtech Soils Ltd, 20 Kenyon Street, Nenagh, Co. Tipperary, Ireland

## **Abstract**

A model is presented for the gravity-driven flow of rainwater descending through the soil layer of a green roof, treated as a porous medium on a flat permeable surface representing an efficient drainage layer. A fully saturated zone is shown to occur. It is typically a thin layer, relative to the total soil thickness, and lies at the bottom of the soil layer. This provides a bottom boundary condition for the partially saturated upper zone. It is shown that after the onset of rainfall, well-defined fronts of water can descend through the soil layer. Also the rainwater flow is relatively quick compared with the moisture uptake by the roots of the plants in the roof. In a separate model the exchanges of water are described between the (smaller-scale) porous granules of soil, the roots and the rainwater in the inter-granule pores.

# 1 Introduction

Green roofs are becoming increasingly popular around the world. The many benefits of a green roof include assistance in the management of storm water, pollution control, building insulation, recycling of carbon dioxide, in addition to being aesthetically pleasing. A green roof is subject to various stresses from the weather, in particular wind-loading, which we ignore in this report, and rainfall: it is the flow, drainage and uptake of rainwater that we model. An understanding of where the water goes is essential to design a roof able to achieve sustained healthy plants and loads that lie within the safe capacity of the supporting structure.

The main focus of this report is on the transport of water through the green roof structure. Inadequate drainage can lead to the undesirable occurrence of a fully saturated soil which will cut off the air supply to the plants. Conversely, if the saturation levels are too low plants will die from lack of water. Ideally a degree of saturation that is less than eighty per cent should be maintained at all times. Our goal is to model the distribution of the degree of saturation through the depth of the soil layer, and to see how it changes due to spells of rain, and under the influence of moisture-uptake by plant roots.

The basic structure of a common green roof is shown in Fig. 1. A waterproof root barrier protects the underlying roof structure. A drainage layer sits atop this barrier. The typical thickness of this layer is 8/15/20 mm depending on the type of roof. The soil and drainage layers are separated by a thin sheet of perforated hard plastic containing holes approximately 2 mm in diameter and spaced 2 cm apart. There are two layers of soil at the top of the structure separated by a layer of felt. A thin layer ( $< 2$  cm) of refined rooting soil contains the plant life, mainly sedum for thinner roofs and, for thicker ones, low growing grasses such as common bent grass and/or other plants, such as cowslip and ladies bedstraw. Beneath the rooting soil are pellets of lightweight expanded clay. This layer is 5-10 cm thick. Grain sizes are typically  $< 2$  mm for rooting soil and 4-8 mm for expanded clay pellets.

## 2 The Model

We model the dynamics of water flow through the soil layer. We consider a single soil layer with thickness  $L \approx 10^{-1}$  m and we ignore the presence of the felt layer. We assume that the soil-drainage-layer interface is located at  $z = 0$  and the soil surface at  $z = L$ . We consider two possible scenarios: (i) the entire region  $0 \leq z \leq L$  is unsaturated, so that the soil saturation  $S$  is always less than 1 and (ii) a saturated region forms at the bottom of the soil layer for  $0 \leq z \leq h$ . Note that the model as presented here is one-dimensional, and represents a horizontal roof, but can be easily extended to two (or three) dimensions, and to account for sloping roofs.

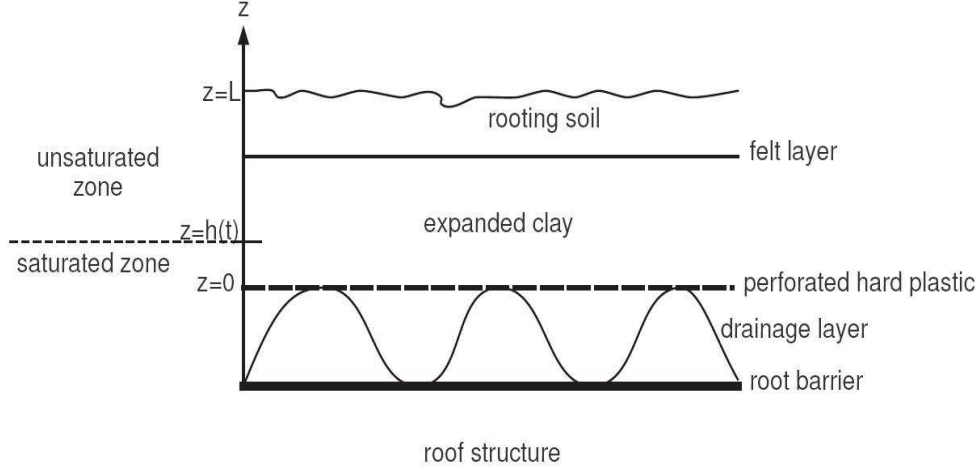


Figure 1: Green roof structure.

## 2.1 The Unsaturated Region

We first assume the entire region  $0 \leq z \leq L$  is unsaturated ( $S < 1$ ). The basic model for this region follows that outlined in [1] and [2]. The one-dimensional Richards' equation for water flow in the unsaturated soil is

$$\phi \frac{\partial S}{\partial t} = \frac{\partial}{\partial z} \left( D_0 D(S) \frac{\partial S}{\partial z} + K_0 K(S) \right) - R, \quad (2.1)$$

where  $S = S(z, t)$ ,  $\phi$  is the constant porosity of the soil, taken here to be 0.25,  $D_0 D(S)$  and  $K_0 K(S)$  are the water diffusivity and hydraulic conductivity respectively, with the functions  $D(S)$  and  $K(S)$  given by

$$K(S) = S^{1/2} [1 - (1 - S^{1/m})^m]^2, \quad (2.2)$$

$$D(S) = \frac{[1 - (1 - S^{1/m})^m]^2}{S^{1/m - 1/2} (1 - S^{1/m})^m}, \quad (2.3)$$

where  $0 < m < 1$ . The value of  $m$  for the expanded-clay soil was not known but, for later use in simulations and analysis of the model, was taken to be  $m = \frac{1}{2}$ . Likewise the values of the constants  $K_0$ , the conductivity for saturated soil, and  $D_0$ , a representative value of diffusivity, were not known. The water flux in the  $z$  direction is  $q = -(D_0 D(S) S_z + K_0 K(S))$ . Water uptake by the plant roots is incorporated into the model through the last term in (2.1) and is given by

$$R = 2\pi a k_r l_d (p_a - p_c f(S) - p_r), \quad (2.4)$$

where  $k_r$  is the radial conductivity of water,  $a$  is the root radius,  $l_d$  is the root length density,  $p_a$  is atmospheric pressure,  $p_r$  is an effective pressure in the roots (although it can be negative),  $p_c f(S)$  is the capillary pressure in the soil, with  $p_c$  another constant characterising the partly saturated pellets, and

$$f(S) = (S^{-\frac{1}{m}} - 1)^{1-m}. \quad (2.5)$$

We take parameter values from Roose and Fowler [2] and let  $2\pi\alpha k_r = 7.85 \times 10^{-16} \text{ m}^2 \text{ s}^{-1} \text{ Pa}^{-1}$ ,  $l_d = 5 \times 10^3 \text{ m}^{-2}$  and  $p_c = 10^4 \text{ N m}^{-2}$ . The root pressure  $p_r$  will be determined from conservation of water within the root. Finally we must prescribe boundary conditions at the top and bottom of the soil layer. At the soil surface we take

$$D_0 D(S) \frac{\partial S}{\partial z} + K_0 K(S) = Q_{\text{in}}(t) \quad \text{at } z = L, \quad (2.6)$$

where  $Q_{\text{in}}$  is the rainfall rate averaged over the surface area of the ground. We assume, in this unsaturated case, no outflow at the base of the soil layer and set

$$D_0 D(S) \frac{\partial S}{\partial z} + K_0 K(S) = 0 \quad \text{at } z = 0. \quad (2.7)$$

We nondimensionalise the equations by scaling

$$z = L\hat{z}, \quad p_r = |P|\hat{p}_r, \quad t = \frac{L}{K_0}\hat{t}, \quad p = p_a + p_c\hat{p}, \quad R = 2\pi\alpha k_r l_d |P|\hat{R}, \quad Q_{\text{in}} = Q_{\text{typ}}\hat{Q}, \quad (2.8)$$

where  $P$  is the (negative) root pressure at the soil surface and we set  $|P| = 10^6 \text{ N m}^{-2}$ . The time scale used here is that for flow through the soil layer under the action of gravity. The dimensionless Richards' equation (2.1) then has the form

$$\phi \frac{\partial S}{\partial \hat{t}} = \frac{\partial}{\partial \hat{z}} \left( \delta D(S) \frac{\partial S}{\partial \hat{z}} + K(S) \right) - \eta(\theta - \varepsilon f(S) - \hat{p}_r), \quad (2.9)$$

where

$$\delta = \frac{D_0}{LK_0} \approx 10^{-4}, \quad \eta = \frac{2\pi\alpha k_r l_d |P|L}{K_0} \approx 4 \times 10^{-6}, \quad \theta = \frac{p_a}{|P|} \approx 10^{-1}, \quad \varepsilon = \frac{p_c}{|P|} \approx 10^{-2}. \quad (2.10)$$

Roose and Fowler [2] give values of  $D_0$  for different soil types and we can reasonably take  $D_0 = 10^{-6} \text{ m}^2 \text{ s}^{-1}$ . However, the value of  $K_0$  is more difficult to determine as it varies significantly with different soil types. The parameter values in (2.10) are given for  $K_0 = 10^{-1} \text{ m s}^{-1}$ . We note that  $\eta \ll 1$  suggesting that water uptake by the roots is negligible over the chosen timescale. The dimensionless forms of the boundary conditions are given by

$$\delta D(S) \frac{\partial S}{\partial \hat{z}} + K(S) = \nu \hat{Q} \quad \text{at } \hat{z} = 1, \quad (2.11)$$

$$\delta D(S) \frac{\partial S}{\partial \hat{z}} + K(S) = 0 \quad \text{at } \hat{z} = 0, \quad (2.12)$$

where

$$\nu = \frac{Q_{\text{typ}}}{K_0} \approx 3 \times 10^{-6}, \quad (2.13)$$

with  $Q_{\text{typ}}$  taken to be some typical rainfall. We set  $Q_{\text{typ}} = 3 \times 10^{-7} \text{ m s}^{-1}$  for a "wet day" in Ireland.

## 2.2 The Saturated Region

When the soil becomes saturated we assume that a moving boundary forms at  $z = \mathbf{h}(\mathbf{t})$  and the soil saturation is identically one for  $z \in [0, \mathbf{h}]$ . Our governing equation can now be written in the (dimensionless) form

$$\frac{\partial}{\partial \hat{z}} \left( 1 + \frac{1}{\gamma} \frac{\partial \hat{p}}{\partial \hat{z}} \right) - \eta (\theta + \varepsilon \hat{p} - \hat{p}_r) = 0, \quad (2.14)$$

where

$$\gamma = \frac{\rho g L}{p_c} \approx 10^{-1}. \quad (2.15)$$

The flux through the membrane at  $z = 0$  is prescribed to occur at a rate proportional to the pressure difference across it;  $Q_{\text{mem}} = \kappa(p - p_a)$  dimensionally, where  $p_a$  is the atmospheric pressure in the drainage layer beneath,  $p$  is the pressure at  $z = 0$ , and  $\kappa \approx 10^{-5} \text{ m s}^{-1} \text{ Pa}^{-1}$  (determined experimentally in the next sub-section). This gives the dimensionless condition

$$1 + \frac{1}{\gamma} \frac{\partial \hat{p}}{\partial \hat{z}} = \alpha \hat{p} \quad \text{at} \quad \hat{z} = 0, \quad (2.16)$$

where  $\alpha = \frac{\kappa p_c}{K_0} \approx 1$ . At the saturation front  $\hat{z} = \hat{\mathbf{h}}(\hat{\mathbf{t}}) \equiv \frac{\mathbf{h}(\mathbf{t})}{L}$ ,  $\hat{p} = 0$  (atmospheric), and continuity of fluid flux requires

$$K(S) + \delta D(S) \frac{\partial S}{\partial \hat{z}} = 1 + \frac{1}{\gamma} \frac{\partial \hat{p}}{\partial \hat{z}} \quad \text{at} \quad \hat{z} = \hat{\mathbf{h}}. \quad (2.17)$$

Neglecting the  $\eta$  term in (2.14) for this saturated region, and using  $\hat{p} = 0$  at  $\hat{z} = \hat{\mathbf{h}}$  along with (2.16), gives

$$\hat{p}(\hat{z}, \hat{\mathbf{t}}) = \frac{\gamma(\hat{\mathbf{h}}(\hat{\mathbf{t}}) - \hat{z})}{1 + \alpha \gamma \hat{\mathbf{h}}(\hat{\mathbf{t}})}, \quad (2.18)$$

so that (2.17) becomes

$$K(S) + \delta D(S) \frac{\partial S}{\partial \hat{z}} = \frac{\alpha \gamma \hat{\mathbf{h}}}{1 + \alpha \gamma \hat{\mathbf{h}}} \quad \text{at} \quad \hat{z} = \hat{\mathbf{h}}. \quad (2.19)$$

In principle equation (2.19) and boundary condition  $S = 1$  at  $\hat{z} = \hat{\mathbf{h}}(\hat{\mathbf{t}})$  determine  $\hat{\mathbf{h}}$  in terms of the flux from the unsaturated region. However, we can simplify things if we notice from (2.11) that the dimensionless flux will in general be small, of order  $\nu$  (due to the rainfall). If this is the case, then the value of  $\hat{\mathbf{h}}$  required to satisfy (2.19) will be small. Physically, this is because for the typical size of fluid flux considered, the pressure required to force it through the membrane according to (2.16) is provided by the hydrostatic head of a very thin layer of water (dimensionally,  $\mathbf{h}$  is calculated to be much less than 1 mm).

Thus if a saturated region is created at the bottom of the soil layer, it will quickly grow to a depth which is sufficient to drain exactly the same amount of water through the membrane as

is arriving from the unsaturated region above. Provided this depth is substantially less than the depth of the soil, the saturated region can be ‘collapsed’ (mathematically) onto the line  $\hat{z} = 0$ , and the boundary condition applied to the problem in the unsaturated zone for some of the numerical solutions of sub-section 2.5 is then

$$\frac{\partial}{\partial \hat{z}} \left[ K(S) + \delta D(S) \frac{\partial S}{\partial \hat{z}} \right] = 0 \quad \text{at} \quad \hat{z} = 0, \quad {}^{11} \quad (2.20)$$

which states that whatever flux arrives there from above is allowed through the membrane (the build-up of the small saturated layer which would physically enable this is therefore assumed to happen instantaneously), with the uptake of water by the roots being neglected. We apply (2.20) while  $K(S) + \delta D(S) \frac{\partial S}{\partial \hat{z}} > 0$  at  $\hat{z} = 0$  since water is trying to exit, not enter, the soil layer.

### 2.3 Experimental measurement of $\kappa$

The value of  $\kappa$  was deduced from a simple experiment, which involved puncturing a 2 mm diameter hole in a plastic bottle, made with material similar to what we believe the drainage membrane is made of. The rate of drainage through the hole driven by the hydraulic head in the bottle was measured, and used to determine the coefficient of proportionality between pressure difference across the membrane  $\Delta p$  and the water flux through it  $q$ . Writing

$$q = \kappa \Delta p, \quad (2.21)$$

where  $\Delta p = \rho g h$ , the water depth in the bottle,  $h$ , satisfies the equation

$$A_{\text{bottle}} \frac{dh}{dt} = -\kappa \rho g h, \quad (2.22)$$

where  $A_{\text{bottle}}$  is the cross-sectional area of the bottle. Thus

$$\log h = -\frac{\kappa \rho g}{A_{\text{bottle}}} t. \quad (2.23)$$

Measurements of  $h$  against  $t$  made during the experiment are in Fig. 2, and the best fit value of the time constant  $t_c = A_{\text{bottle}}/\kappa \rho g$  was 74 seconds. The flux through an individual hole can be converted into an average velocity through a membrane, using the area of the membrane  $A_{\text{membrane}}$  that is drained by each hole. Thus

$$\bar{u} = \kappa \Delta p, \quad \kappa = \frac{A_{\text{bottle}}}{A_{\text{membrane}} \rho g t_c}. \quad (2.24)$$

Taking  $A_{\text{membrane}} = \pi \text{ cm}^2$ , and using the cross-sectional area of the bottle  $A_{\text{bottle}} = 25 \text{ cm}^2$ ,  $\rho = 10^3 \text{ kg m}^{-3}$ , and  $g = 10 \text{ m s}^{-2}$ , gives  $\kappa \approx 10^{-5} \text{ m s}^{-1} \text{ Pa}^{-1}$ .

---

<sup>11</sup>More accurately the bottom condition might be specified in linear complementary form  $(1 - S)q = 0$  with  $1 - S \geq 0$  (for no super-saturation) and  $q \leq 0$  (for upward flux). We use (2.20) for its convenience in some of the numerical simulations, but for others we approximate the more correct linear complementary form, as in (2.33).

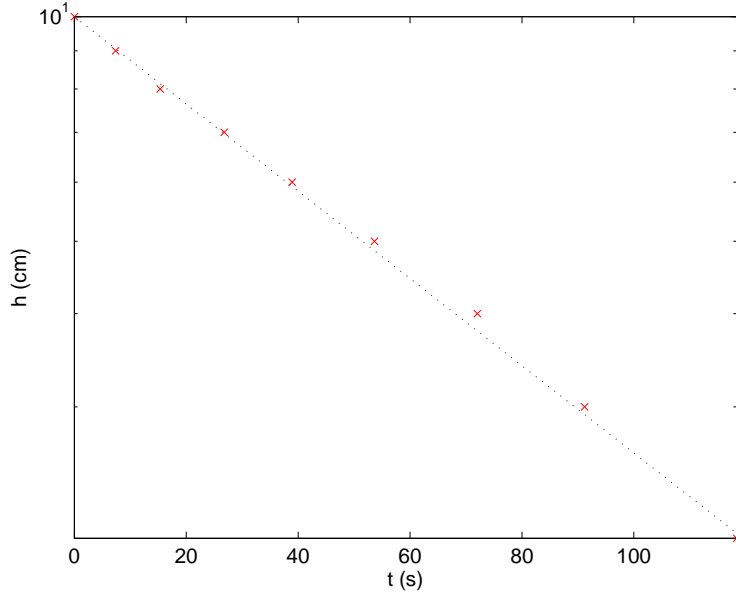


Figure 2: Experimental measurements of  $h$  against  $t$ .

## 2.4 The Root Pressure

To determine the root pressure  $p_r$  in equation (2.9), we assume that the root extends through the full thickness of the soil layer of depth  $L$ . Conservation of water inside the root yields

$$k_z \frac{d^2 p_r}{dz^2} + 2\pi\alpha k_r (p_a - p_c f(S) - p_r) = 0, \quad (2.25)$$

where  $k_z = 10^{-14} \text{ m}^6 \text{ s}^{-1} \text{ N}^{-1}$  is the root axial conductivity and  $f(S)$  is defined in equation (2.5). Zero axial flux at the root tip implies

$$\frac{dp_r}{dz} + \rho g = 0 \quad \text{at} \quad z = 0. \quad (2.26)$$

In addition we prescribe a driving pressure at the root base yielding

$$p_r = p_a + P \quad \text{at} \quad z = L. \quad (2.27)$$

In dimensionless form the root pressure will satisfy

$$\frac{d^2 \hat{p}_r}{d\hat{z}^2} + \tau (\theta - \varepsilon f(S) - \hat{p}_r) = 0, \quad (2.28)$$

subject to

$$\frac{d\hat{p}_r}{d\hat{z}} = -\varepsilon\gamma \quad \text{at} \quad \hat{z} = 0, \quad (2.29)$$



$$\hat{p}_r = \theta - 1 \quad \text{at} \quad \hat{z} = 1, \quad (2.30)$$

where

$$\tau = \frac{2\pi\alpha k_r L^2}{k_z} \approx 10^{-3}. \quad (2.31)$$

The parameters  $\tau \ll 1$  and  $\varepsilon\gamma \ll 1$  which implies  $\frac{d^2\hat{p}_r}{d\hat{z}^2} \approx 0$  subject to  $\frac{d\hat{p}_r}{d\hat{z}} = 0$  on  $\hat{z} = 0$ . The root pressure is thus given by

$$\hat{p}_r = \theta - 1. \quad (2.32)$$

The complete model is now given by (2.9), with the definitions (2.2), (2.3), (2.5) and (2.32), with boundary condition (2.11) at  $\hat{z} = 1$  and (2.12) if  $S < 1$ , or (2.20) if  $S = 1$ , at  $\hat{z} = 0$ . An initial condition is also needed.

The diffusion term in (2.9) is small, so the equation is essentially a first order non-linear wave equation; the boundary condition (rainfall) is transmitted downwards as a wave. If rain starts suddenly, there is a shock front that propagates quickly down to the bottom of the soil; if it stops suddenly there is an expansion fan.

## 2.5 Numerical Solutions

The governing equation for the unsaturated region (2.9) was solved subject to boundary conditions (2.11) and (2.12). As a first approach the  $\eta$  term in (2.9) is neglected so that we are just considering drainage of the soil layer under gravity. The initial saturation was taken to be uniform throughout the soil layer. Three different initial values of the saturation  $S_{\text{init}} : 0.05, 0.1, 0.15$  were considered. The profiles obtained for  $S$  in each case when the computation was stopped are shown in Fig. 3; a corresponding semilog plot is shown in Fig. 4, in order to demonstrate the boundary layer of thickness  $\delta^{1/2}$  in  $S$  at  $\hat{z} = 0$  that is predicted by an asymptotic analysis, and which is captured by the numerical solution, but which is not visible in Fig. 3. For  $S_{\text{init}} = 0.1$  and  $0.15$ , computations were stopped when the value of  $S$  at  $\hat{z} = 0$ ,  $S_{\text{bottom}}$ , reached 1; for  $S_{\text{init}} = 0.05$ ,  $S_{\text{bottom}}$  is still far from 1, even for the value of dimensionless time (100) shown here. The time evolution of  $S_{\text{bottom}}$  is shown in Fig. 5, while that for  $S$  at  $\hat{z} = 1$ ,  $S_{\text{top}}$ , is shown in Fig. 6.

Thus, the results suggest an appreciable difference in the time at which complete saturation is achieved at the bottom of the soil when  $S_{\text{init}}$  is increased from 0.05 to 0.1. The effect of the rainfall boundary condition (2.11) has (by the end of the simulations) only affected the tiny region at the right of Fig. 3, where there is the beginning of a shock front propagating downwards from  $\hat{z} = 1$ ; since  $\delta$  has been taken to be very small, the shock looks very sharp, and the values on either side of it are the initial condition (below, or left, of the shock), and the value given by  $K(S) = \nu\hat{Q}$  (above, or right, of the shock - this value is expectedly independent of the initial condition, as shown in Fig. 6).

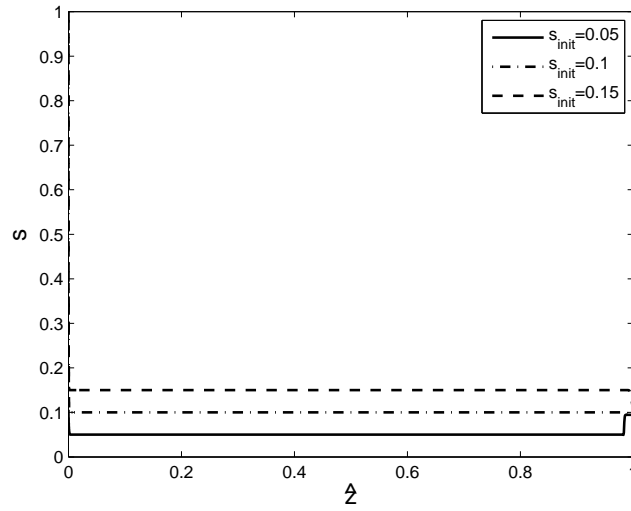


Figure 3:  $S$  vs.  $\hat{z}$  for three different initial conditions ( $S_{\text{init}} = 0.05, 0.1, 0.15$ ) at either dimensionless time 100 ( $S_{\text{init}} = 0.05$ ) or when  $S$  reaches 1 at  $\hat{z} = 0$  ( $S_{\text{init}} = 0.1, 0.15$ ). Parameter values are  $m = 1/2$ ,  $\delta = 10^{-4}$ ,  $\nu = 3 \times 10^{-6}$ .

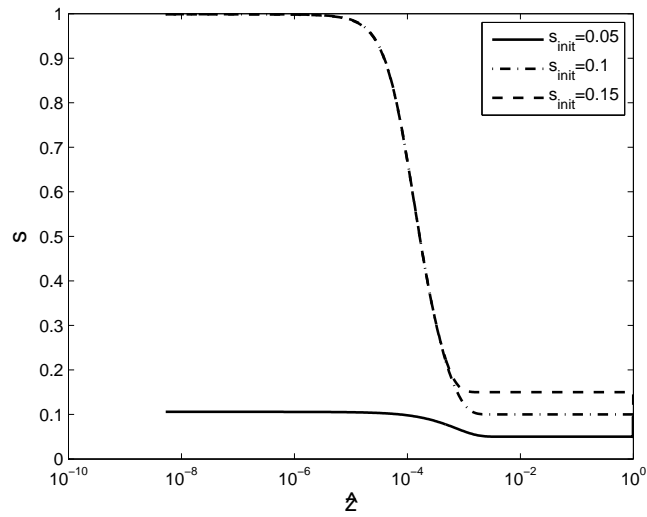


Figure 4: A semilog plot of  $S$  vs.  $\hat{z}$  for three different initial conditions ( $S_{\text{init}} = 0.05, 0.1, 0.15$ ) at either dimensionless time 100 ( $S_{\text{init}} = 0.05$ ) or when  $S$  reaches 1 at  $\hat{z} = 0$  ( $S_{\text{init}} = 0.1, 0.15$ ). Parameter values are  $m = 1/2$ ,  $\delta = 10^{-4}$ ,  $\nu = 3 \times 10^{-6}$ .

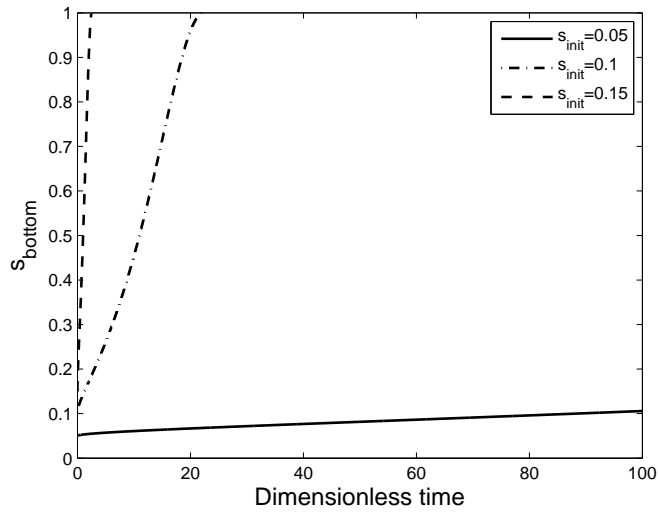


Figure 5:  $S_{\text{bottom}}$  vs. dimensionless time for three different initial conditions ( $S_{\text{init}} = 0.05, 0.1, 0.15$ ). Parameter values are  $m = 1/2$ ,  $\delta = 10^{-4}$ ,  $\nu = 3 \times 10^{-6}$ .

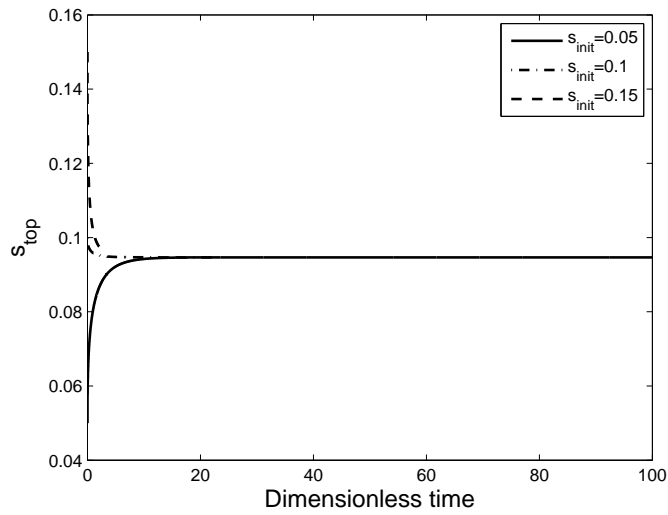


Figure 6:  $S_{\text{top}}$  vs. dimensionless time for three different initial conditions ( $S_{\text{init}} = 0.05, 0.1, 0.15$ ). Parameter values are  $m = 1/2$ ,  $\delta = 10^{-4}$ ,  $\nu = 3 \times 10^{-6}$ .

The complete problem, with a small saturated region allowed for by using boundary condition (2.20), and with  $\eta \neq 0$ , was also solved by discretising in space and solving with the method of lines using `ode15s` in Matlab. To apply the switch in boundary conditions smoothly, the condition

$$q_0 = q_1 e^{-1000(1-S)}, \quad (2.33)$$

was applied for the flux at the bottom node  $q_0$  in terms of the flux at the node above  $q_1$ ; thus when  $S$  is close to 1 this becomes  $\partial \hat{q} / \partial \hat{z} = 0$ , and when  $S$  is less than 1 it becomes  $q_0 = 0$ . The diffusion coefficient is infinite when  $S = 1$ , but this does not cause any issues in the numerics, possibly because the above boundary condition ensures  $S$  never quite reaches 1.

This seems to allow for steady states when rainfall is constant; if there is more rainfall than is taken up by the roots, the saturation at the bottom is 1 and there is a boundary layer of width  $\delta^{1/2}$  in which it adjusts to the value as determined by  $K(S) \approx v\hat{Q} - \eta \int_0^L R$  (Fig. 7). If there is less rainfall than is taken up by the roots, the saturation at the bottom decreases almost to 0.

Fig. 7 shows the result of a sudden increase in rainfall from  $\hat{Q} = 0.1$  to  $\hat{Q} = 10$ , which shows the initial shock front travelling down into the soil and the eventual steady state. The saturation at the bottom does not increase towards 1 until the shock front arrives there. Fig. 8 shows the result of a sudden decrease back to  $\hat{Q} = 0.1$ . Note that the time intervals shown are longer; there is an initial expansion fan on the timescale of the gravity drainage which reduces the saturation to the value given by  $K(S) = v\hat{Q}$ , followed by a slower decay (on the timescale  $O(\frac{1}{\eta})$ ) as the roots take up the remaining water.

### 3 Two-Porosity Model

The expanded clay pellets used in green roof construction are quite large but contain lots of pore space. The difference in pore sizes between these, and the inter-pellet space means water can be drawn into the pellets and retained there for longer than it would otherwise remain in the soil. Thus a two-porosity model would seem appropriate.

This is an outline of a ‘‘box’’ or ‘‘lumped’’ model for water storage in the macro-pores between soil particles, which have saturation  $S$ , and in the micro-pores within the particles, which have saturation  $S_p$ . Transport of water into or out of the particles is parameterised to occur at a rate proportional to the saturation difference  $S - S_p$ .<sup>12</sup> The roots do not penetrate into individual particles so provide a sink term  $R$  only from the macro-pores. This root uptake  $R(S)$  is primarily due to the large negative pressure in the root system, but as saturation decreases a large capillary pressure acts to counteract this; thus  $R(S)$  is roughly constant for  $S$  close to 1 but decreases at small  $S$  (as in the model above).

---

<sup>12</sup>A variant of this model might assume that water transfer into the particles occurs at a rate proportional to the *pressure* difference  $p_{cP}f(S_p) - p_c f(S)$ ; since the capillary pressure in the micropores would be larger than in the macropores ( $p_{cP} > p_c$ ), this would cause more water to be transferred into the micropores, and a larger supply would be maintained there for the roots to take up.

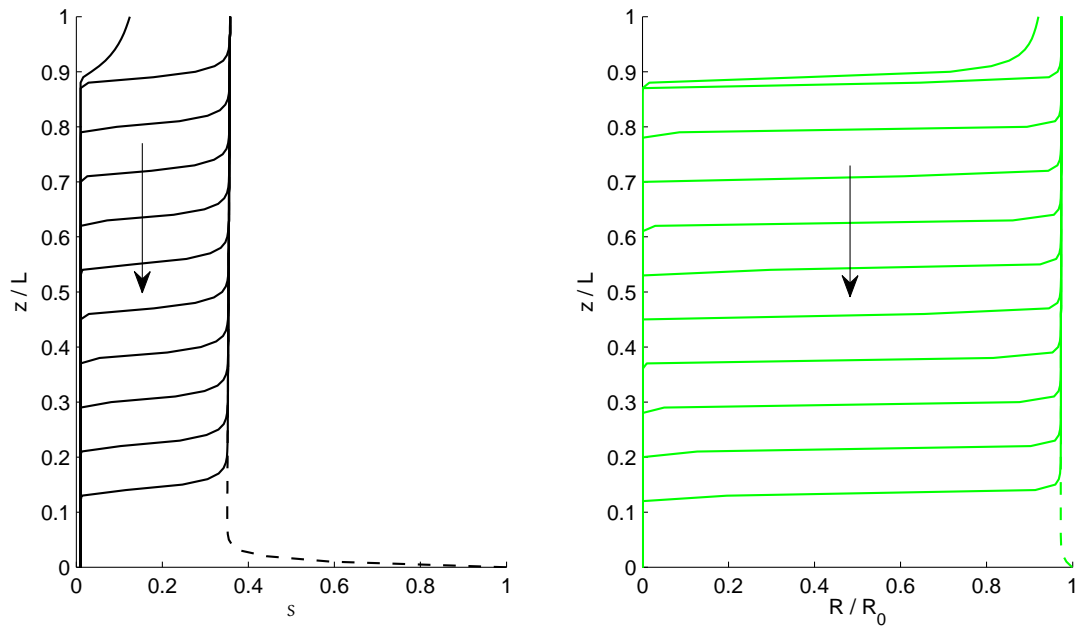


Figure 7: Profiles of saturation and root uptake at time intervals of 1 (in the dimensionless units); the arrow shows the direction of increasing time. This is the result of a sudden increase in rainfall to  $\hat{Q} = 10$ , from the steady state when  $\hat{Q} = 0.1$ , and the dashed line shows the steady state that results. Parameter values are  $m = 1/2$ ,  $\delta = 10^{-2}$ ,  $\eta = 4 \times 10^{-4}$ ,  $\nu = 3 \times 10^{-4}$ ,  $\varepsilon = 10^{-2}$ ,  $\gamma = 10^{-1}$ .

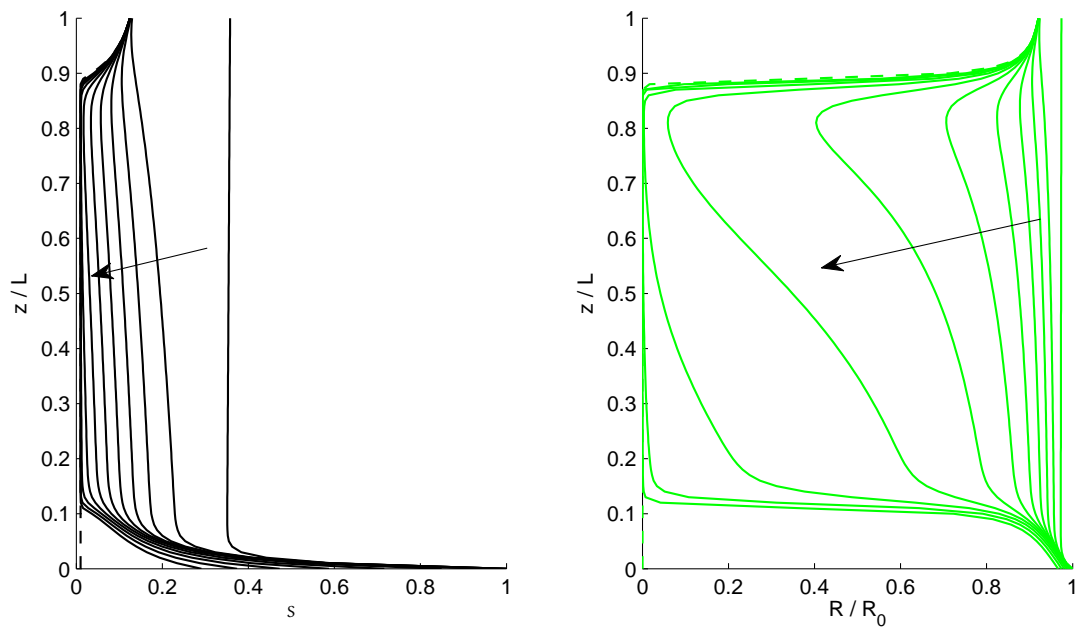


Figure 8: Profiles of saturation and root uptake at time intervals of 10 (in the dimensionless units); the arrow shows the direction of increasing time. This is the result of a sudden decrease in rainfall from  $\hat{Q} = 10$ , to  $\hat{Q} = 0.1$ . Parameter values are  $m = 1/2$ ,  $\delta = 10^{-2}$ ,  $\eta = 4 \times 10^{-4}$ ,  $\nu = 3 \times 10^{-4}$ ,  $\varepsilon = 10^{-2}$ ,  $\gamma = 10^{-1}$ .

The following equations are dimensionless, and the time scale has been chosen to be that due to uptake by the roots (the time scale differs from that used previously by a factor  $\eta$ ). Drainage from the volume of soil is supposed to occur due to gravity at a rate  $K(S)$ , and occurs on a time scale  $\eta$  compared to the uptake by the roots (see above). Rainfall provides a source which is scaled to be the same size as the gravity drainage (note this is different to above - the scale for the rainfall here is large and is intended to represent the size of heavy showers; the dimensionless  $r(\hat{t})$  will be 0 most of the time, when it is not raining, and  $O(1)$  when it is raining heavily).

$$\phi \frac{dS}{d\hat{t}} = \frac{1}{\eta} r(\hat{t}) - \frac{1}{\eta} K(S) - \lambda(S - S_p) - R(S), \quad (3.1)$$

$$(1 - \phi) \phi_p \frac{dS_p}{d\hat{t}} = \lambda(S - S_p), \quad (3.2)$$

where  $r = v\hat{Q}$ ,  $\phi_p$  is the porosity of the pellets and

$$K(S) = S^{1/2} [1 - (1 - S^2)^{1/2}]^2, \quad (3.3)$$

which comes from equation (2.2) with  $m = \frac{1}{2}$  and

$$R(S) = 1 - \varepsilon \frac{(1 - S^2)^{1/2}}{S}. \quad (3.4)$$

The use of  $K(S)$  for the gravity drainage in equation (3.1) is motivated by the fact that the water flow in the earlier part of the report is (since  $\delta$  is small) essentially determined by this hydraulic conductivity. The time scale for water to diffuse into individual particles is estimated using their dimensions  $L_p \sim 1$  cm and a diffusion coefficient  $D_p \sim 10^{-9}$  m<sup>2</sup> s<sup>-1</sup>.  $L_p^2/D_p$  is comparable to the time scale for uptake by the roots ( $\sim 10^5$  s), so the parameter  $\lambda$  is order 1. In equation (3.1)  $\eta$  is very small and in equation (3.4)  $\varepsilon$  is also small, and we consider especially the distinguished case  $\varepsilon \sim \eta^{2/7}$ .

The behaviour of solutions to this model is quite straightforward, and an example solution for a large rain storm followed by dry weather is in Fig. 9. When it is raining,  $r$  is order 1, and on a fast time scale,  $\hat{t} \sim O(\eta)$ , the saturation  $S$  relaxes towards the equilibrium given by  $K(S) = r(\hat{t})$ . This causes water to then transfer into the particles on an  $O(1)$  time scale according to (3.2). By balancing terms in equation (3.1) we seek a similarity solution for small  $S$  for which  $K(S) \approx \frac{1}{4} S^{\frac{9}{2}}$ . When it stops raining  $r = 0$ , and the saturation  $S$  decreases quickly due to gravity drainage on an  $O(\eta)$  time scale; approximately

$$\phi \frac{dS}{d\hat{t}} \sim \frac{1}{\eta} K(S). \quad (3.5)$$

Thus, neglecting the small  $O(\eta^{\frac{2}{7}})$  terms suggests  $S$  tends towards 0 as

$$S \sim \left( \frac{2\phi\eta}{7\hat{t}} \right)^{2/7}. \quad (3.6)$$

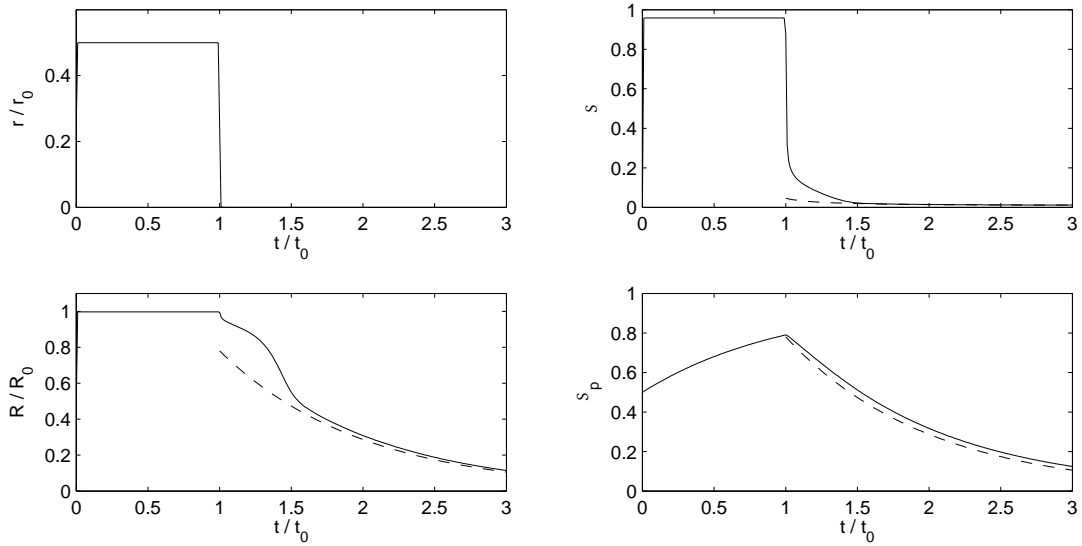


Figure 9: Solutions for macro-scale and particle-scale saturations  $S$  and  $S_p$ , and root uptake  $R$ , as a result of rainfall  $r(t)$  which represents a large rain shower. Dashed lines show the limiting behaviour. Parameter values are  $\eta = 10^{-4}$ ,  $\lambda = 1$ ,  $\varepsilon = 10^{-2}$ .

On the  $O(1)$  time scale, therefore,  $S \sim \eta^{2/7}$ , and the equations are

$$O(\eta^{2/7}) = O(\eta^{2/7}) - \lambda(O(\eta^{2/7}) - S_p) - \left(1 - \frac{\varepsilon}{S}\right), \quad (3.7)$$

$$(1 - \phi)\phi_p \frac{dS_p}{d\hat{t}} = \lambda(O(\eta^{2/7}) - S_p). \quad (3.8)$$

Thus, ignoring the  $O(\eta^{2/7})$  terms,  $S_p$  decays exponentially and the water coming out into the macropores is immediately taken up by the roots:  $R = \lambda S_p = -(1 - \phi)\phi_p dS_p/d\hat{t}$ , as shown in figure 9. Root uptake is maintained for a much longer period after it ceases to rain than would be the case with no micropores, when  $S$  decreases rapidly towards 0.

### 3.1 A Model for Fast Saturation

Assuming instead fast saturation of the pellets,

$$S_p = S_0 H(S), \quad (3.9)$$

where  $H$  denotes the Heaviside function,  $S_p$  denotes the saturation of the individual pellets,  $S_0$  is the porosity of an individual pellet, and  $S$  is the saturation of the inter-pellet pores. The required short time scale can arise from high capillary pressures associated with the very small pores within the pellets.



Taking now  $\phi = \frac{1}{4}$  to be the total proportion of space occupied by air and water within the soil, and  $S_O = \frac{1}{5}$ , the inter-pellet porosity is  $\varphi = \frac{1}{16}$  (given by  $\varphi + \frac{1}{5}(1 - \varphi) = \frac{1}{4}$ ). Equation (2.9) can then be replaced by

$$\frac{1}{16} \frac{\partial}{\partial \hat{t}} (S + 3H(S)) = \frac{\partial}{\partial \hat{z}} \left( K(S) + \delta D(S) \frac{\partial S}{\partial \hat{z}} \right) - \eta \hat{R}, \quad (3.10)$$

with  $\hat{R} \sim 1$ , from (2.9) and (2.32). (Equation (3.10) might be better written in terms of the total water content,  $S_T = \frac{1}{16}(S + 3H(S))$ , so that  $S$  on the right-hand side is replaced by  $S(S_T) = 0$  for  $0 \leq S_T \leq \frac{3}{16}$ ,  $S(S_T) = 16(S_T - \frac{3}{16})$  for  $\frac{3}{16} \leq S_T \leq \frac{1}{4}$ .)

Where the pellets are saturated,  $S > 0$  and  $H(S) = 1$ , the equations are as in Section 2. Here, for simplicity, an initially dry soil is considered, so that at  $\hat{t} = 0$ ,  $S \equiv S_p \equiv 0$ . For  $\hat{t} > 0$ , a region  $\hat{W}(\hat{t}) < \hat{z} < 1$  has become wet:

$$S = H(S) = 0 \text{ in } 0 < \hat{z} < \hat{W}, \quad S > 0 \text{ and } H(S) = 1 \text{ in } \hat{W} < \hat{z} < 1. \quad (3.11)$$

To obtain an order-one sized wet region, the relevant time scale must be that for the rainfall (days) so that time has to be rescaled:

$$\hat{t} = \tilde{t}/\nu. \quad (3.12)$$

Note that this time scale is similar to that for the up-take of water by the plants' roots. It is also appropriate, from the top boundary condition, to rescale the saturation:

$$S = \nu^{2/9} \tilde{S}, \quad (3.13)$$

where, since we have assumed that  $m = \frac{1}{2}$ ,  $K(S) \sim \frac{1}{4}S^{9/2}$  and  $D(S) \sim \frac{1}{4}S^{5/2}$  for small  $S$ .

Neglecting the time-derivative term (now effectively of order  $\nu^{2/9}$ ), the partial differential equation becomes

$$\frac{1}{4} \frac{\partial}{\partial \hat{z}} \left( \tilde{S}^{9/2} + \tilde{\delta} \tilde{S}^{5/2} \frac{\partial \tilde{S}}{\partial \hat{z}} \right) = \tilde{\eta} \hat{R}. \quad (3.14)$$

Here  $\tilde{\eta} = \eta/\nu \approx \frac{1}{3}$  and  $\tilde{\delta} = \delta/\nu^{2/9} \approx \frac{1}{600}$ , using the values of Section 2. Although the value of  $\tilde{\delta}$  is small here, because of the uncertainty in the values of the physical parameters describing water transport through the soil, it could conceivably be of order one and it is therefore retained in (3.14), for the present.

The differential equation is subject to the top boundary condition

$$\frac{1}{4} \left( \tilde{S}^{9/2} + \tilde{\delta} \tilde{S}^{5/2} \frac{\partial \tilde{S}}{\partial \hat{z}} \right) = \hat{Q}_{\text{in}} \text{ at } \hat{z} = 1 \quad (3.15)$$

and, assuming that the diffusive,  $\tilde{\delta}$ , term is retained, a lower boundary condition

$$\tilde{S} = 0 \text{ at } \hat{z} = \hat{W}(\tilde{t}). \quad (3.16)$$

Finally, to fix the position of the free boundary  $\hat{z} = \hat{W}(\hat{t})$  between dry and wet soil, conservation of mass of water at this point, where  $S_p$  jumps from 0 to  $S_O$ , leads to

$$\frac{d\hat{W}}{d\hat{t}} = -\frac{4}{3} \left( \tilde{S}^{9/2} + \tilde{\delta} \tilde{S}^{5/2} \frac{\partial \tilde{S}}{\partial \hat{z}} \right) \text{ at } \hat{z} = \hat{W}(\hat{t}). \quad (3.17)$$

(Since, for  $\tilde{\delta} > 0$ ,  $\tilde{S} = 0$  at this point, the second term on the right-hand side should then be interpreted as  $\tilde{\delta} \lim_{\hat{z} \rightarrow \hat{W}} \left\{ \tilde{S}^{5/2} \frac{\partial \tilde{S}}{\partial \hat{z}} \right\}$ .)

Of course, if the pellets were already partially saturated, (3.17) would be suitably modified, leading to a faster-moving free boundary.

Note also that if the diffusion can be neglected, (3.14) and (3.15) lead to  $\frac{1}{4} \tilde{S}^{9/2} = \hat{Q}_{in} + \hat{z} - 1$  so (3.17) gives

$$-\frac{d\hat{W}}{d\hat{t}} = \frac{16}{3} (\hat{Q}_{in} + \hat{W} - 1). \quad (3.18)$$

The free-boundary condition (3.17) only applies for an advancing wet region,  $d\hat{W}/d\hat{t} \leq 0$ . An alternative form is needed for when this region contracts, which will happen when the rainfall decreases sufficiently. In any part of the soil between the lowest location of the free boundary and its current position, the roots can continue to remove water from the pellets, thereby reducing  $S_p$ .

As described in this report we could now have at least four types of region within the soil layer:

1. Dry zone, where  $S = S_p = 0$ ;
2. Damp or moist (unsaturated) zone I, where  $S = 0$ ,  $0 < S_p < S_O$ ;
3. Damp or moist (unsaturated) zone II, where  $0 < S < 1$ ,  $S_p = S_O$ ;
4. Wet (saturated) zone, where  $S = 1$ ,  $S_p = S_O$ .

## 4 Conclusions

In this report a one-dimensional time dependent mathematical model has been described for the development of the saturation in the soil layer of a flat green roof. Our model suggests that a fully-saturated ( $S = 1$ ) region forms at the base of the soil layer and this region can be thin relative to the total soil thickness.

From an initial dry state and from the onset of persistent rain, fronts of saturation were computed to descend through the layer. The decrease of saturation from unity following a decrease in rainfall was also described. The end result is that most of the rainwater falls through the soil layer and exits through the network of holes in the bottom supporting sheet.

On a smaller scale, the pellets and soil particles are themselves porous and made up of micropores. The water flow in and out of a typical particle is modelled using the flux between (a) the macropores (whose saturation is as modelled above) and (b) the root system. This two-porosity model suggests that during the time between spells of rain the micropores can retain (for long periods of time) water that is available to be taken up by the roots.

Further work might include adapting the soil thickness  $L$  to rainfall at the site of the building with the aim of making  $L$  as small as possible, while avoiding problems with saturation and aridity. A first step towards this goal would be to carry out experiments to more accurately determine the values of the constants. Further simulations using more extensive rainfall data could then be carried out to determine the optimum soil thickness. In addition small modifications could be made to include the influence of a sloped roof.

## **Acknowledgements**

We acknowledge the support of the Mathematics Applications Consortium for Science and Industry ([www.macsi.ul.ie](http://www.macsi.ul.ie)) funded by the Science Foundation Ireland mathematics initiative grant 06/MI/005.

# Bibliography

- [1] M. T. Van Genuchten. A closed-form equation for predicting the hydraulic conductivity of unsaturated soil. *Soil Sci. Soc. Am. J.*, 44:892-898, 1980.
- [2] T. Roose and A.C. Fowler. A model for water uptake by plant roots. *J. Theoret. Biol.*, 228:155-171, 2004.